Automatic image analysis of multicellular apoptosis process

Riccardo Ziraldo, Nichole Link, John Abrams and Lan Ma

***Abstract*— Apoptotic programmed cell death (PCD) is a common and fundamental aspect of developmental maturation. Image processing techniques have been developed to detect apoptosis at the single-cell level in a single still image, while an efficient algorithm to automatically analyze the temporal progression of apoptosis in a large population of cells is unavailable. In this work, we have developed an ImageJ-based program that can quantitatively analyze time-lapse microscopy movies of live tissues undergoing apoptosis with a fluorescent cellular marker, and subsequently extract the temporospatial pattern of multicellular response. The protocol is applied to characterize apoptosis of *Drosophila* wing epithelium cells at eclosion. Using natural anatomic structures as reference, we identify dynamic patterns in the progression of apoptosis within the wing tissue, which not only confirms the previously observed collective cell behavior from a quantitative perspective for the first time, but also reveals a plausible role played by the anatomic structures in *Drosophila* apoptosis.**

I. Introduction

Apoptosis, a form of programmed cell death (PCD), is an orderly cellular process whereby damaged or unnecessary cells are destroyed and removed in a programmed manner. Apoptotic removal of unnecessary cells is employed throughout tissue remodeling and organ development of *Drosophila* fruit fly, a powerful model organism for the study of developmental apoptosis [1]. In this study, we focus on the developmental process of *Drosophila* wings regulated by apoptosis. At eclosion, the hatching stage of the adult fly from the pupal case, the collapsed wing structure expands to its maximum size. In the meantime, the epithelial cells undergo apoptosis, and the debris is removed, leaving the wing structure transparent, except at the location of the veins. Considerable efforts have been made to elucidate the apoptosis process, particularly at single-cell level, using quantitative experimentation [2]. Nevertheless, little effort has been taken to explore the apoptosis response across a population of cells, and the current investigation of the plausibly collective apoptotic response at multicellular level remains in the form of intuitive observations [3]. Notably, a lack of quantitative tools to analyze cell-population data has limited our ability to extract temporal and spatial characteristics of the process. Previous studies on image processing of apoptotic cellular response mainly analyze single frames instead of tracking the progression of cells over an extended time period [4-7]. In this work, we have studied an application of image analysis techniques to the automatic quantification of spatiotemporal evolution of the apoptosis process of *Drosophila* wing at tissue level, measured by in vivo time-lapse fluorescence microscopy. The designed image analysis algorithm is able to identify and segment fluorescence-labeled nuclei of single cells from image sequences. Subsequently, each nucleus is temporally tracked and checked for morphological changes that reveal the onset of apoptosis. With the use of geometric reference maps, plausible spatiotemporal patterns of the progression of apoptosis across the tissue can finally be detected.

R. Ziraldo and L. Ma are with the Department of Bioengineering, University of Texas at Dallas, Richardson, 75080 TX, USA (corresponding author e-mail: lan.ma@utdallas.edu).

N. Link is with the Department of Molecular and Human Genetics, Baylor College of Medicine, Houston, 77030 TX, USA

J. Abrams is with the Department of Cell Biology, UT Southwestern Medical Center, Dallas, 75390 TX, USA.

II. Methods

A. Overview of algorithm

The current algorithm is developed for, but not limited to, analysis of time-lapse video microscopy of *Drosophila* wing epithelium with fluorescent nuclear marker (Movie 1, at http://utdallas.edu/~lan.ma/Movie1.tif). Experimentally, a transgenic nuclear DsRed reporter (vg:DsRed) has been used to monitor the apoptosis progression [3]. In viable cells, the vg:DsRed protein is localized to the nucleus. When a cell undergoes apoptosis, the integrity of the nuclear envelope is compromised and the fluorescent protein is released into the cytosol. The main goal of this work is to quantify a temporal and spatial pattern, if any, of the multicellular apoptosis process. In this regard, we have designed a two-phase image analysis algorithm implemented by the ImageJ framework, a versatile image processing freeware widely utilized by the biochemical community (http://rsbweb.nih.gov/ij/).

The workflow of the algorithm is illustrated in Figure 1, where the numbered arrows refer to the data output at each step, starting from the original microscopy movie as input (Figure 1, arrow 1). In Phase One, the image sequence is initially checked for data quality and consistency through a preprocessing step, including removal of obstructed frames, registration of misaligned frames, and a standard sharpening filter for signal amplification. Note that the wing veins and edge are not affected by the apoptosis process, and thus are masked in the preprocessing step and excluded from further analysis. The preprocessed images (Figure 1, arrow 2) are then subject to the step of fluorescence localization, where the signal is classified into nuclear, cytosolic, or background fluorescence. The resulting data (Figure 2, arrow 3) is displayed in a two-color map showing the location of the nucleus as well as the cytosolic leakage, which is further utilized to detect the morphology of single cells, in Phase Two. Meanwhile, the preprocessed image sequence undergoes a cell tracking algorithm [8], whose output contains a temporal series of coordinate sets for each cell.

In Phase Two, morphology measurements of the nuclear areas detected in Phase One is performed first. It has been shown that changes in the morphology of the cell nucleus can be used to determine the onset of apoptosis [6, 7]. The morphology data (Figure 2, arrow 4) is then combined with

978-1-4244-7929-0/14/$26.00 ©2014 IEEE

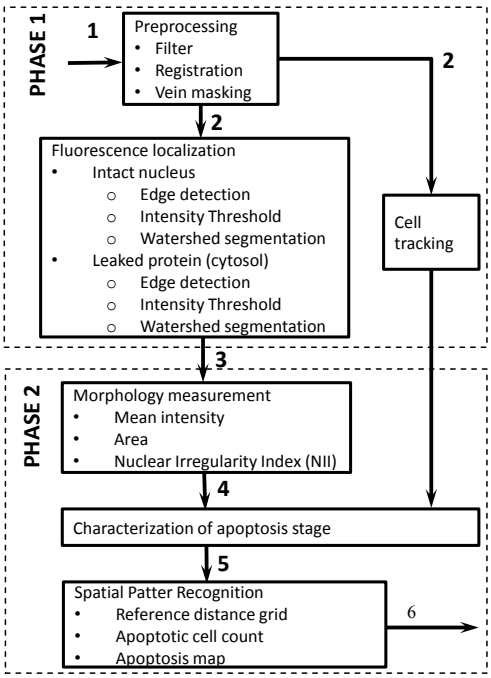

Figure 1. Workflow of the image processing algorithm.

the temporal coordinates to determine the progression of apoptosis in each cell, by the step of 'characterization of apoptosis stage'. The resultant output (Figure 2, arrow 5) is a color-coded apoptosis map showing the position of each cell and its apoptosis state (viable or apoptotic). To identify plausible communal patterns of multicellular PCD in the wing, each apoptosis map in a temporal sequence is divided into equivalent regions according to the anatomical quadrants of the wing. In each region, the fraction of apoptotic cells is calculated, to quantify the degree of apoptosis at multicellular level. Finally, to visualize the temporospatial evolution of PCD in the wing, the two-dimensional distribution of the degree of apoptosis is plotted as a time-lapse color map (Figure 2, arrow 6). In the following subsections, we will discuss in greater detail the steps after preprocessing.

B. Fluorescence localization

The fluorescent signal of cells may be classified into three distinct biological states: in state one, the nuclear envelope is intact; in state two, the nucleus with partial membrane is surrounded by cytosolic leakage of the reporter protein; in state three, nuclear membrane is not detectable while the reporter protein is completely cytosolic. States two and three correspond to apoptotic cells, while only state one corresponds to live cells. In terms of fluorescent appearance, the intact nucleus has relatively high fluorescence intensity and a sharp edge. In contrast, the cytosolic fluorescence has relatively low intensity with a dull outer edge. Therefore, edge sharpness together with pixel intensity is chosen as criteria to segment and classify the two types of fluorescent localization, nuclear and cytosolic.

First, a Canny-Deriche edge detector is applied to the preprocessed images (Figure 2, arrows 2) to detect the position of the nuclear envelope of live cells. Secondly, an intensity threshold is determined under the guidance of the detected nuclear edges. Specifically, a binary map of nuclear edges is overlaid on the corresponding preprocessed image as a visual guidance, and then the user can select an appropriate value of cut-off threshold to ensure that only pixels above the threshold as well as encircled by the nuclear edge are selected as intact cellular nuclei. Those isolated fluorescent areas with pixel intensities above the selected threshold, but not surrounded by detected edges, are not considered intact nuclei. The resultant data are binary images delineating the location of the intact nuclei in the original images. Thirdly, in the case of touching nuclei appearing in the binary image, the domain occupied by a single cell and the position of its cell border are estimated using a watershed algorithm.

Once the location of intact nuclei is determined, the nuclear pixels are removed from the preprocessed image, and the remaining fluorescence is, presumably, attributed to cytosolic leakage of the reporter protein and background. Then the same three steps used to segment intact nuclei, namely edge detection, intensity thresholding and watershed segmentation, are used in this step of classification. All the remaining pixels are considered as background signal.

C. Characterization of the apoptosis stage

In Phase Two, we identify each cell to be viable or dead (apoptotic). We find it is challenging to precisely determine the initial time point of cytosolic leakage if we solely rely on the fluorescence localization (data not shown). Rather, we need to take into account further characteristics of apoptosis, such as the morphological changes in the shape and size of the nucleus, as previously described, which have proven more effective in identifying cellular apoptosis [6, 7].

In particular, during the temporal evolution of apoptosis three cellular stages with distinct morphological features can be defined. In the first stage, the nucleus is intact with stable size, normal mean fluorescence intensity as well as a regular shape, and the cell is considered viable (denoted as 'Vi'). In the second stage, the nucleus is characterized by shrinking size, increased mean intensity and regular shape, and is considered to be in a compacted stage (denoted as 'Co), during which a cell prepares for nuclear condensation of apoptosis [9]. In the final stage, the fluorescent area, composed of a dismantled nucleus plus cytosolic leakage, or cytosolic protein only, has a larger area and a decreased average intensity due to cytosolic dispersion, and the cell is considered apoptotic (denoted as 'Ap'). To classify cells into these three defined apoptotic stages, we need to quantify morphological features from the fluorescence localization map. In this regard, Filippi-Chiela et al. describes two morphological parameters, nuclear area (denoted as 'A') and the nuclear irregularity index (denoted as 'NII'), a composite measure of several shape descriptors [7]. With the images used here, we find that a third parameter, mean fluorescent intensity (denoted as 'I'), is helpful in efficiently identifying the three cellular stages. The reason is because compacted chromatin in the Co stage results in increased concentration of the reporter protein and hence enhanced mean fluorescent signal, in contrast to cells in the Ap stage with lower average intensity as the nuclear protein disperses into cytosol.

Furthermore, instead of setting independent parametric criteria for each stage, we only need to characterize the Co stage, which has the most prominent nuclear features to recognize, and in addition temporally separates the Vi and Ap

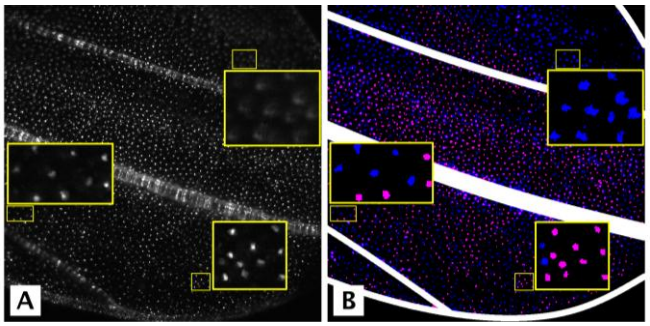

Figure 2. Comparison of the two-color map of detected nuclear and cytosolic area (B) with the original image (A). In (B), the nuclear area is colored in magenta, while the cytosolic area is colored in blue. Three insets including 31 cells are correspondingly shown in (A) and (B) for comparison.

stages. For a single cell, once the frame of the Co stage is determined, the preceding and succeeding frames can be identified as Vi and Ap stage, respectively. Specifically for the Co stage, we expect to see a combinatorial feature with decreased nuclear area (A), highest mean fluorescence intensity (I) and regular shape (NII) [6, 7]. For practical considerations, additional lower bounds for A and the NII and an upper bound for the mean intensity are also needed as biologically attainable limits, to excludes outliers that are not cellular, such as fluorescent areas that are too small to be a nucleus, and areas with saturating pixel intensity. The logic rule to determine the Co stage is then expressed as follows:

$$(I_{min} \le I \le I_{max}) AND (A_{min} \le A \le A_{max}) AND (NII_{min} \le NII \le NII_{\max})$$

If any of the three parametric criteria is not satisfied, the cell is considered to be either in the Vi stage or the Ap stage, depending on its temporal order relative to the Co frame.

D. Temporal apoptosis analysis

Using the positions found by the cell-tracking algorithm, the progression of the apoptosis stage of single cells can be followed over time. We assume that the entrance of a cell into the Co stage is irreversible, meaning that once a viable cell transits into the Co stage, it has to enter the Ap stage in later frames. Therefore, for the cells fluctuating in and out of the Co stage, the first time the nucleus enters the Co stage and the last time it exits the Co stage are defined as the beginning and end of the Co stage, respectively. The result of temporal analysis is stored as a series of binary map showing the apoptosis stage (live or apoptotic) of each cell in each frame. In particular, cells in the Vi or Co stage are considered as alive while cells in the Ap stage are considered apoptotic.

E. Spatial pattern determination

The progression of apoptosis is analyzed according to the natural reference system of the wing anatomy, such as the veins and the hinge, as we hypothesize that they play a role in regulating apoptosis, either through the delivery of chemical signals, or providing specific hydrostatic impact on the epithelium. To extract spatial patterns according to our hypothesis, the wing is first divided into major quadrants based on salient anatomical features, including the veins, the edge and the hinge of the wing. Each quadrant is then geometrically sliced according to the distance from selected anatomic structures as boundary. The choice of anatomical features to divide the wing may be modified at the user's discretion. A same distance grid is applied to all the frames to monitor the evolution of plausible collective pattern. A value representing the percentage of single cells in the Ap stage out of the population residing in a sliced domain is assigned to each slice, and further plotted as a color map. The time-lapse sequence of apoptosis color map is the final output.

III RESULTS AND DISCUSSION

It is noteworthy that the microscopy images used here are captured to include the largest possible wing area, with the purpose of analyzing the apoptosis patterns at the tissue level. This compromises on the magnification level, leaving the original nuclei roughly visible at single-cell level. Therefore, one challenge here is the difficulty to discern nuclear signal from cytosolic signal based on images with relatively low sub-cellular resolution. We find that the sequential segmentation of the nuclei and cytosolic region of single cells can help detect the relatively dimmer signal of the cytosolic leakage of reporter protein, with higher accuracy as well as efficiency. An example of the segmented nuclear and cytosolic localization map is shown in Figure 2.

In Figure 3, the time trajectories of the three morphological parameters of five cells are shown. In addition, the color maps indicating the Vi, Co or Ap stage of each cell are illustrated using the same color scheme.

To check if our program can correctly detect the apoptotic

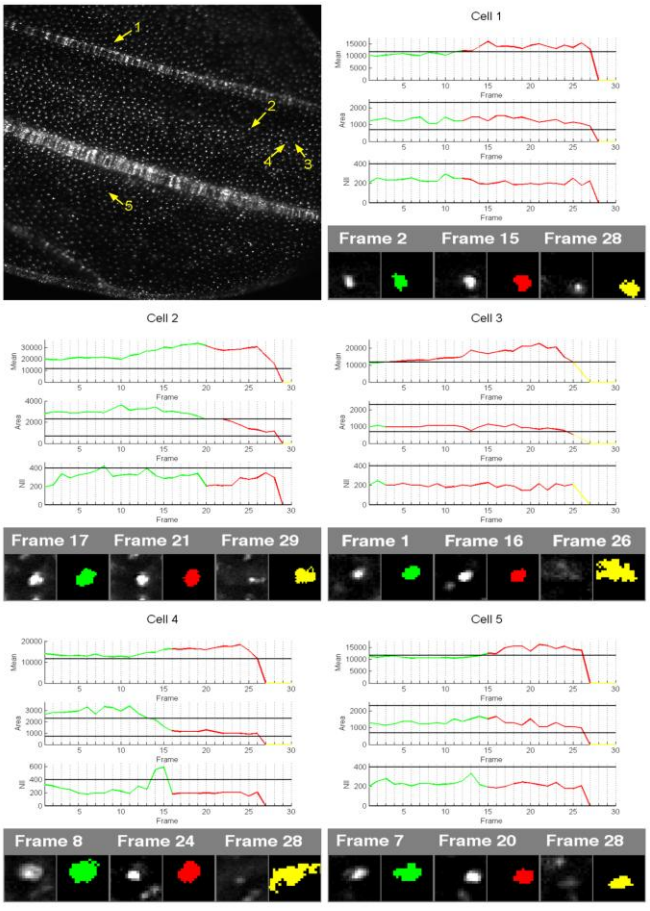

Figure 3. Temporal change of the three morphology parameters, A (area), I (mean intensity) and NII (nuclear irregularity indenx) of 5 cells and detection of their apoptotic status. The segmented cells and their trajectories are marked in red if all the criteria of the Co stage are satisfied, or in green if the frame precedes the Co stage, or in yellow if the frame follows the Co stage.

status of single cells, we perform subjective counting of apoptotic cells in a sub-region including 200 cells, and then compare the result with that from the program detection. The false positive and false negative rate averaged for the image sequence is 0.6% and 4.4%, respectively, suggesting that the detection of apoptotic cells by the program is reliable.

Our approach of spatial pattern recognition can quantify propagation of apoptosis in relationship to the anatomical structure of the Drosophila wing over an extended time span. Figure 4 shows examples of macroscopic apoptosis patterns across the wing tissue based on five different reference grid maps (denoted as ALL, NV, CV, E, H). Note that an anatomical structure is either marked in magenta if it is used as a reference boundary in the pattern analysis, or in white if it is not. As a result, we can recognize temporospatial pattern of apoptosis response, even though there exist some degree of stochasticity in that the propagation along a certain direction may fluctuate back and forth between neighboring slices.

In particular, the ALL map in Figure 4 shows a trend of communal apoptosis process starting along slices near the veins and edge, which then gradually propagates towards the center of each quadrant. In addition, apoptosis in the top quadrant starts intensively from the location near the wing hinge. Such pattern indicates that plausibly a biochemical signal triggering the initiation of apoptosis is released from the veins, edge as well as the hinge of the wing and subsequently diffuses towards the center of the quadrant. Note that in this regard the main longitudinal vein appears to have a lesser effect than the other veins, in that cells close to it undergo PCD in a much more delayed time scale than those close to other veins. This collective pattern of propagation starting from the veins, the edges and the hinge is again evident in the NV case (Figure 4), where the thick central vein is excluded from the reference system. In the CV case, the pattern also suggests that the central main vein has a lesser effect in inducing cellular apoptosis compared to the other two veins and the edge. That is, the collective wave of apoptosis most intensively starts from locations near the thinner veins and edge. Thus we speculate that the pro-apoptosis biochemical signal may be more diluted in, or released more slowly from the central main vein. In the E and H cases, the resulting apoptosis map not only confirms the propagation pattern from the edge toward the center of the wing as observed above, but also a concomitant pattern from two ends towards the midline along the longitudinal axis of the wing, indicating that cellular apoptosis may additionally be up-regulated by mechanical force induced by the cuticle fusion process, which generally starts from the outer edge of the wing and moves towards the body. The same collective pattern of apoptosis is reproducibly obtained from the analysis of second set of video microscopy data (Movie 2 at http://utdallas.edu/~lan.ma/Movie2.tif, apoptosis map of Movie2 http://utdallas.edu/~lan.ma/Movie2_ApopMap.zip).

III. Conclusion

The new image processing program is capable of high-throughput analysis of sequences of fluorescent images, each containing a large number of cells (>10^3). The temporal evolution of the spatial distribution of the apoptotic activity across local tissue regions can be displayed as a sequence of color maps, enabling visualization of the dynamic tissue-level behavior.

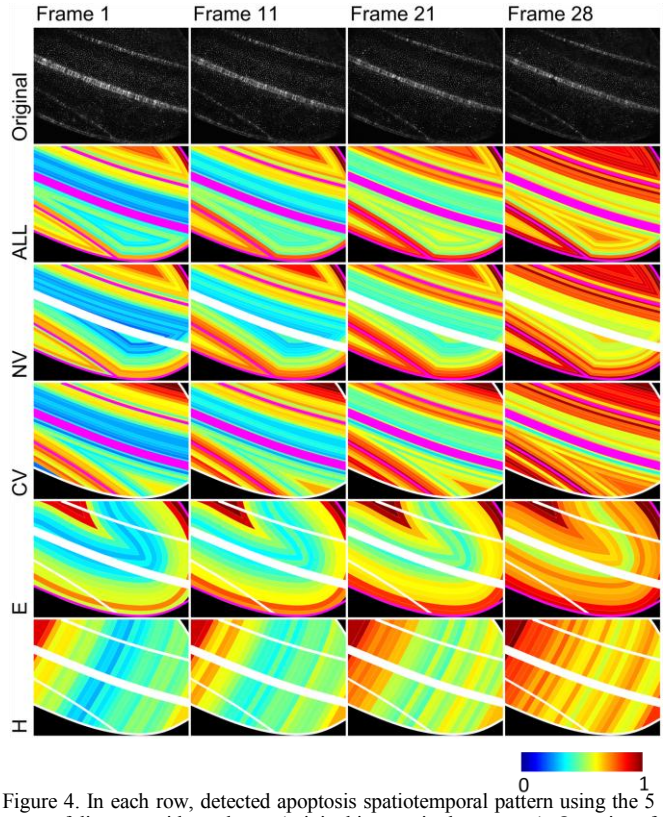

Figure 4. In each row, detected apoptosis spatiotemporal pattern using the 5 types of distance grid are shown (original images in the top row). On strips of the distance grid, the numbers of apoptotic cells normalized to the total numbers of cells, (valued between 0 and 1), and are plotted in each frame as a color map using the color scale given at the bottom.

Acknowledgment

The authors would like to thank the Start-up Fund from the University of Texas at Dallas, and also acknowledge the assistance of the UT Southwestern Live Cell Imaging Facility, a Shared Resource of the Harold C. Simmons Cancer Center, supported in part by an NCI Cancer Center Support Grant, P30CA142543.

References

[1] H. Steller. "Regulation of apoptosis in Drosophila" *Cell Death and Differentiation*, vol. 15, pp. 1132–38, 2008.

[2] S.L. Spencer and P.K. Sorger. "Measuring and modeling apoptosis in single cells". Cell 144(6), pp. 926-39, 2011.

[3] N. Link, P.Chen, W. Lu, K. Pogue, A. Chuong, M. Mata, J. Checketts, J. Abrams. "A collective form of cell death requires homeodomain interacting protein kinase". *J Cell Biol* 178(4), 567-574, 2007.

[4] J.W.Navalta,R. Mohamed, A. El-Baz, B.K. McFarlin, and T.S. Lyons. "Exercise-induced immune cell apoptosis: image-based model for morphological assessment". Eur J Appl Physiol 110, 325-331, 2010.

[5] I.M. Helmy, and A.M. Azim. "Efficacy of ImageJ in the assessment of apoptosis". Diagn Pathol 7: 15, 2012.

[6] M. DeCoster. "The Nuclear Area Factor (NAF): a measure for cell apoptosis using microscopy and image analysis". In: Mendez-Vilas, A., Diaz, J. (eds.) Modern Research and Educational Topics in Microscopy, pp. 378-84.

[7] E. Filippi-Chiela, M. Oliveira, B. Jurkovski, S. Callegari-Jacques, V. da Silva, G. Lenz, G. "Nuclear Morphometric Analysis (NMA): Screening of Senescence, Apoptosis and Nuclear Irregularities". PLoS ONE 7(8), 42522, 2012.

[8] I. Sbalzarini and P. Koumoutsakos. "Feature point tracking and trajectory analysis for video imaging in cell biology". Journal of Structural Biology 151(2), pp. 182-195, 2005.

[9] Ura, S., Nishina, H., Gotoh, Y., Katada, T. "Activation of the c-Jun N-terminal kinase pathway by MST1 is essential and sufficient for the induction of chromatin condensation during apoptosis". Molecular and cellular biology 27(15), 5514-22, 2007.